Core–mantle boundary heat flow

The Earth can be viewed as a massive heat engine, with various energy sources and sinks. Insights into its evolution can be obtained by quantifying the various energy contributions in the context of the overall energy budget. Over the past decade, estimates of the heat flow across the core–mantle boundary, or across a chemical boundary layer above it, have generally increased by a factor of 2 to 3. The current total heat flow at the Earth's surface — 46 ± 3 terawatts (10^{12} J s^{-1}) — involves contributions from heat entering the mantle from the core, as well as mantle cooling, radiogenic heating of the mantle from the decay of radioactive elements, and various minor processes such as tidal deformation, chemical segregation and thermal contraction gravitational heating. The increased estimates of deep-mantle heat flow indicate a more prominent role for thermal plumes in mantle dynamics, more extensive partial melting of the lowermost mantle in the past, and a more rapidly growing and younger inner core and/or presence of significant radiogenic material in the outer core or lowermost mantle as compared with previous estimates.

THORNE LAY[1]*, JOHN HERNLUND[2] AND BRUCE A. BUFFETT[3]

[1]Earth and Planetary Sciences Department, University of California, Santa Cruz, California 91125, USA; [2]Earth and Ocean Sciences, University of British Columbia, Vancouver, British Columbia, Canada, V6T 1Z4; [3]Department of Geophysical Sciences, University of Chicago, Chicago, Illinois 60637, USA

*e-mail: thorne@pmc.ucsc.edu

Energy is one of the most fundamental parameters of the Earth's physical system, but it is difficult to determine robustly. The most accessible integrative energy measure for the planet is the total amount presently released at the surface, mainly comprising heat conducted through the surface rocks and from volcanic activity and hydrothermal circulation. Direct global measurements of heat conduction based on thermal gradients in shallow boreholes with calibrated rock-sample thermal conductivities indicate a total of 30–32 terawatts (TW), which increases to 43–49 TW when corrected according to an ocean lithosphere thermal model that accounts for observational underestimation due to hydrothermal circulation[1,2]. Although there has been some debate about the half-space cooling models used to correct the observations, the arguments for an upper value of 46 ± 3 TW appear sound. Crustal concentrations of radioactivity are estimated to account for 6–8 TW (out of ~20 TW of radiogenic heating in the chondritic model for the bulk silicate Earth)[2], with some estimates of depleted upper-mantle radiogenic heat generation (~2 TW) and cooling (~3 TW), leaving as much as 33–35 TW that should be passing from the lower mantle to the upper mantle[3,4].

This large lower-mantle heat flow includes contributions from lower-mantle radiogenic heat generation (~10–12 TW), lower-mantle cooling (5–25 TW) and transfer of heat from the core into the base of the mantle (Fig. 1). Constraining any one source or sink bounds the residual balance. Diverse approaches have been pursued to estimate the heat flux at the core–mantle boundary (CMB), or at least upwards from the lowermost mantle. Early estimates[5–7] gave values in the range 3–4 TW, indicating that there is only minor heating of the mantle from below and that thermal plumes play a secondary role in mantle circulation. Recent estimates, however, have yielded values in the range 5–15 TW from independent considerations of core temperature, geodynamo energetics and buoyancy flux of lower-mantle thermal plumes. Further constraints have recently been provided by direct determinations of the temperature in the lowermost mantle, which were made by relating seismic velocity discontinuities to a laboratory-calibrated phase change in magnesium silicate perovskite ($MgSiO_3$). These findings have important implications for the evolution of the deep Earth.

LOWER-MANTLE TEMPERATURES AND PROPERTIES

Determination of the CMB heat flow requires models for temperature, composition, material properties and/or dynamics of the deep interior, all of which are subject to large uncertainties. Absolute temperatures in the deep mantle are particularly difficult to constrain, and until recently have primarily been approximated by vast extrapolations from calibrated phase boundaries in the transition zone and at the inner-core boundary[8]. Upper bounds on CMB temperatures have been estimated by determinations of the lower-mantle solidus[9–11] and from outer-core melting temperature estimates[10,12], whereas lower bounds are obtained by extrapolating transition-zone temperatures downwards along mantle adiabats (or subadiabats), giving values of 2,500–2,800 K. Allowing for the presence of a thermal boundary layer (TBL), these approaches lead to loosely constrained CMB temperatures (T_{CMB}) of 3,300–4,300 K (Fig. 2), which is a huge range for such an important Earth parameter. Increases of 500–1,800 K in temperature across a 200 km thick superadiabatic TBL with a thermal conductivity of ~10 W m^{-1} K^{-1} predict a net CMB heat flow of 5–13 TW (refs 10,13–15). Thus, relatively hot outermost core temperatures (>3,600 K) consistent with inner-core boundary

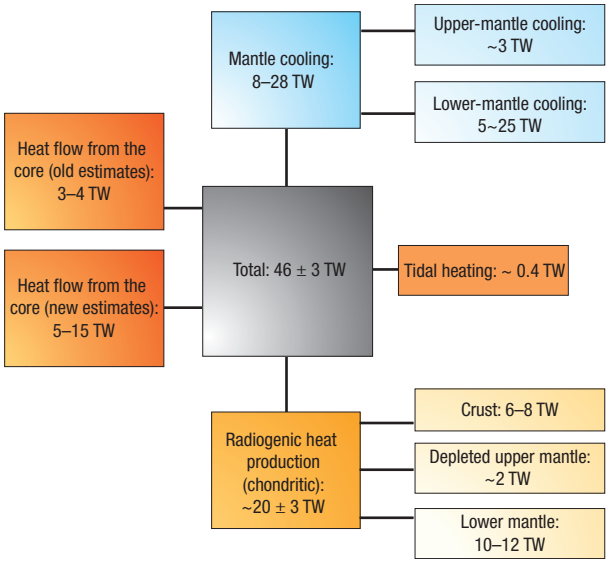

Figure 1 Global heat-flow balance. The primary contributions to observed total surface heat flow (46 ± 3 TW) are shown here. Radiogenic heat production, mantle cooling and heat flow from the core dominate the mantle energy budget, but there are substantial uncertainties in the latter two contributions. Improved constraints on any component will also constrain the balance of the other components. Early estimates of heat flow from the core of 3–4 TW are now being challenged by higher estimates of 5–15 TW, which can bring the sum of heat sources into agreement with the observed heat flow without requiring exceptionally large mantle cooling or non-chondritic radiogenic heat production.

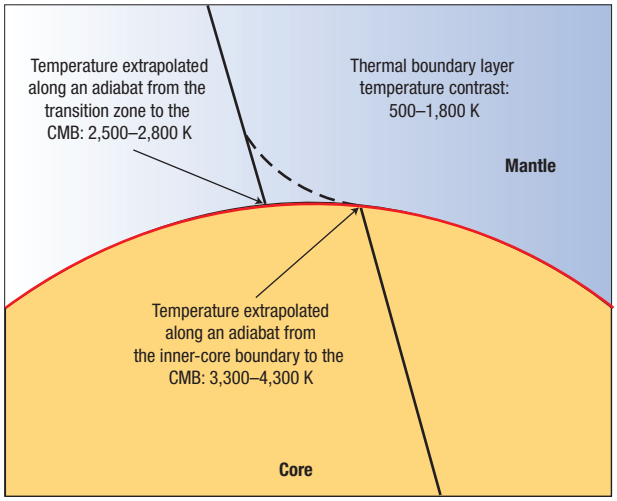

Figure 2 Core–mantle boundary temperature contrast. Temperature contrast at the core–mantle boundary (CMB) 2,891 km deep is constrained by extrapolating laboratory-calibrated temperatures from phase transitions associated with seismic velocity discontinuities in the transition zone (410 km deep) and at the inner core–outer core boundary (5,150 km deep) along mantle and core adiabats, respectively. This results in large estimates of the temperature contrast across the CMB thermal boundary layer. Using a standard value of mantle thermal conductivity, heat flow across the CMB is expected to be in the range 5–13 TW for a simple boundary layer. If there is a stably stratified thermochemical boundary with two thermal boundary layers or a mid-mantle thermal boundary layer, this can be reduced by a factor of two or more.

temperature estimates of 5,300–5,650 K, which now appear to be favoured by iron-melting experiments, indicate relatively high CMB heat-flow values for simple TBL models[12,16,17].

Conductive heat flow depends on temperature gradients and thermal conductivity, which are both very challenging to determine for the deep mantle[14,18] and core[19]. It has been proposed that commonly neglected radiative transport of heat is important for the deep mantle[18], although it seems likely that even minor impurities will inhibit radiative transport. High-pressure transitions from high-spin to low-spin for Fe^{3+} and Fe^{2+} in lower-mantle minerals may also reduce radiative conductivity[20]. Nonetheless, the commonly used estimate of thermal conductivity of 10 W m^{-1} K^{-1} (ref. 14) has at least 50% uncertainty[13].

Seismological, geodynamical and mineral physics observations favour the presence of chemical heterogeneity in the lowermost mantle boundary layer, thought to be a residue from the core-formation process, segregation of dense subducted slab components, effects of partial melting, and/or chemical interactions between the core and mantle[21–23]. The presence of a thermochemical boundary layer (TCBL) should affect present day and early Earth dynamics and heat transport significantly[24–29]. Chemical heterogeneity enhances uncertainties in material properties such as thermal conductivity and thermal expansivity. Inferences of temperature variations and attendant heat flow have large uncertainties as a result.

All estimates of CMB and deep-mantle heat flow require indirect procedures with some assumptions and clever analysis. The primary approaches to estimating deep-mantle heat flow are now discussed, with consideration of uncertainties in key material properties that affect heat-flow estimates. The reliance on indirect inference means there are substantial uncertainties, but the convergence in estimates from independent approaches is encouraging.

GEODYNAMO ENERGETICS

The power available to the geodynamo through convection in the core is ultimately controlled by heat flow into the base of the mantle. Buoyancy at the boundaries of the core, which is generated in response to the CMB heat flow, drives vigorous convection that regenerates the Earth's magnetic field. Much of the work done in generating the field is dissipated through the small, but finite, electrical resistance of the core iron alloy. Estimates of the power dissipated by the geodynamo place bounds on the CMB heat flow because the magnetic field, which would vanish on timescales of 10^4 years in the absence of regeneration by convection, has persisted since at least 3.5 Gyr ago.

Two important sources of buoyancy are produced at the base of the liquid core by growth of the inner core (nominally at a rate of 10^{-3} m yr^{-1}) owing to solidification of the surrounding liquid. One source of buoyancy is generated by exclusion of incompatible light elements from the solid, whereas the other is due to latent heat release (Box 1). Cooling of the core directly sets the pace of both of these buoyancy sources. Cold, dense fluid may also drive convection from the top of the core, but only if the CMB heat flow exceeds the amount of heat conducted along the adiabat in the core. Given the high thermal conductivity of liquid metals, a substantial fraction of the CMB heat flow can be delivered from the core by conduction along the adiabat. Commonly cited estimates for the thermal conductivity near the top of the core[30] yield an adiabatic heat flow of 5–8 TW. A recent downward revision of thermal conductivity[19] suggests a heat flow closer to 3–4 TW, but lower thermal conductivity implies lower electrical conductivity as most heat is probably carried by electrons, and a lower conductivity (higher resistance) could increase the dynamo dissipation.

In principle, the present-day CMB heat flow could be either larger or smaller than the heat flow conducted along the core adiabat. A subadiabatic heat flow would shut off convection at the top of the core, but a broad convective region is still possible because of compositional buoyancy owing to inner-core growth. On the other hand, a superadiabatic heat flow would drive convection from both the top and bottom of the core, sustaining a higher rate of dissipation. Distinguishing between these two possibilities depends on the actual dissipation required to maintain the Earth's magnetic field. Numerical geodynamo models suggest dissipation on the order of 0.1 TW when the structure of the predicted field is scaled to the spatial dimensions of the Earth's core[31]. Attempts to extrapolate model results to Earth-like conditions using an empirical scaling inferred from a suite of numerical models and laboratory studies suggest a dissipation of roughly 0.3 TW (ref. 32). However, numerical models use artificially large diffusivities to suppress small-scale flow. Such small-scale flow is probably present in the Earth's core, and it must contribute to the dissipation. However, the magnitude of this effect is not known. Consequently, we cannot presently rule out the possibility of much higher dissipations (and hence much higher CMB heat flows)[33].

A plausible (but uncertain) dissipation of 1 TW could presently be sustained with a CMB heat flow of 3–4 TW (ref. 31), although viable changes in physical parameters could increase this to 8 TW (ref. 34). This range of heat flow is at or below the adiabatic heat flow, which means that convection is driven entirely by inner-core growth and that a thermally stratified layer might be present in the outermost core. The associated buoyancy sources would have been diminished when the inner core was smaller than at present, so early CMB heat flow would need to have been higher to sustain the same dissipation. Prior to the formation of the inner core, convection was driven solely by thermal buoyancy generated by removal of heat from the top of the core. A heat flow in excess of 13 TW would have probably been required to maintain a dissipation of 1 TW (decreasing the dissipation to 0.5 TW still requires more than 8 TW for the pre-inner core CMB heat flow).

The preceding discussion suggests that subadiabatic heat flow at the CMB is feasible at the present time, but only if CMB heat flow was substantially higher in earlier times to compensate for the smaller size or absence of the inner core. Such large variations in heat flow with time could arise from effects of temperature-dependent viscosity in the mantle, in which case the mantle heat flow would have a strong dependence on Rayleigh number (for example, $Ra^{0.3}$). The heat flow might also vary with time owing to a gradual accumulation of radiogenic material at the base of the mantle[35], which acts to suppress heat flow from the core. A weaker scaling of heat flow with Rayleigh number[36,37] implies that it is more constant over time, which would mean that the present heat flow would have to be higher than believed in order to correspond with values that were needed to sustain the magnetic field over most of the Earth's history. Addition of radiogenic heating in the core demands a further increase in CMB heat flow to produce the same dissipation because the rates of cooling and inner-core growth are reduced[38]. Although a heat flow of 3–4 TW may suffice to sustain the current geodynamo, there are good reasons to suppose that CMB heat flow is much higher.

Less direct constraints on the CMB heat flow could be derived from the radial seismic structure in the boundary region. For example, a thermally stratified layer is expected to develop when the CMB heat flow is subadiabatic[39]. Detection of such a layer would imply low heat flow. Although a region ~12 km thick in the outermost core may have anomalously high seismic velocities[40,41] compatible with the presence of an immiscible iron alloy, most seismic models suggest a slight reduction of velocity in the outermost 50 km of the core[42]. Geomagnetic constraints suggest that any stratified layer is less than 100 km thick[43] but there is no seismic evidence for a thicker thermal stratified zone.

Box 1 Core heat-flow contributions

Cooling of initial heat

Radiogenic heat generation

Gravitational energy from release of light elements during inner-core solidification

Latent heat from inner-core solidification

Change in pressure as core cools

PLUME FLUX CONSTRAINTS

Given that a CMB heat flow of more than 3–4 TW is required for sustaining the geodynamo, there must be a TBL at the base of the mantle with conductive heat transport and a superadiabatic thermal gradient. Seismologically detected inhomogeneity in the lowermost few hundred kilometres of the mantle (the D″ region) has long been attributed to a TBL[5]. Fluid systems partially heated from below can generate hot upwelling TBL instabilities. Thus, the D″ region is regularly invoked as the source of thermal plumes that rise through the mantle and sustain enduring loci of surface volcanism at hotspots. Some level of thermal stratification may exist at the base of the transition zone owing to inhibition of radial flow. However, there is no clear evidence for any alternate mid-mantle TBL that could generate thermal plumes. Although the very existence of mantle-traversing thermal plumes is an area of ongoing debate, heat flux from a hot thermal boundary layer will almost certainly be concentrated in plume upwellings.

Estimation of the buoyancy flux of upwelling plume material required to account for large swells around surface hotspots has been one approach to estimating heat flux through the CMB, following the assumption that mantle-traversing plumes do exist. Estimates of 2–4 TW are obtained from interpreting the dynamic topography sustained by plume tails[6,7,37,44]. Interpreting these values as a full measure of CMB heat flux suggests that only ~10% of the heat transport to the upper mantle is the result of basal heating.

Numerical convection models now indicate several reasons why early plume flux estimates are likely to be underestimates. Some heat goes into warming of the subducted lithosphere in the lower mantle[45], some hot weak plumes never reach the surface[46], and some may be swept into asthenospheric flow[47], with reduced expression in the surface topography (Fig. 3). Attempts to account for these effects increase the estimated CMB heat flux relative to dynamic topography calculations to values of 8–12 TW (ref. 13). Estimates of the plume flux itself may also vary with depth. The excess heat in a plume can be described in terms of an entropy excess, dS, as TdS, where T is temperature. If the entropy excess in a plume is nominally constant, then the heat flow at the CMB will be greater because T is higher. Plume buoyancy flux in the deep mantle is likely to be larger than in the upper mantle owing to the effect of an expected subadiabatic thermal gradient within the convecting mantle[46,48]. Reduction of lower-mantle temperatures by several hundred degrees relative to the adiabat can double the temperature differences between the plumes and surrounding mantle as depth increases, with plume cooling effectively doubling the estimate of plume heat flux to at least 7 TW (ref. 37). Three-dimensional isochemical models with moderately temperature-dependent viscosity[48] give a heat flux of up to 13 TW for all upwellings, whether or not they reach the surface. Computed plume flux estimates remain quite uncertain owing to limitations in modelling temperature-dependence of viscosity[45].

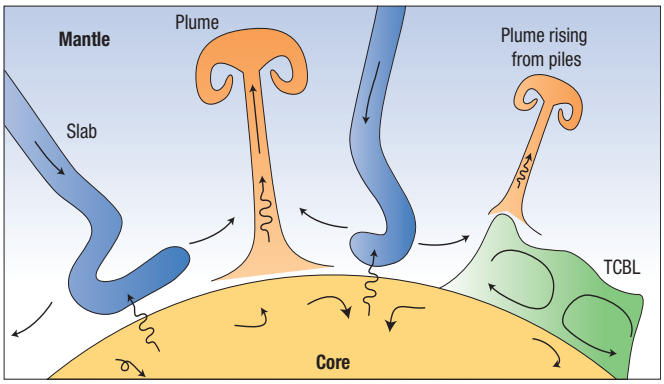

Figure 3 Deep-mantle heat-flow components. Heat conducts non-uniformly across the CMB, with high heat flux into regions of low-mantle temperature, a portion of which heats subducted cooled slabs or downwellings, whereas some may eventually rise in thermal plumes. Radiogenic heating may be concentrated in a thermochemical boundary layer (TCBL), swept into piles. Internal heating of diffuse radiogenic materials also occurs. The variable heat flux at the CMB strongly affects turbulent convection in the core.

Another reason to revise the plume heat flux inferred from dynamic topography is that chemical buoyancy may play a role in addition to thermal buoyancy. A TCBL, possibly enriched in heat-producing materials, is commonly proposed for the D″ region. Numerical models of thermochemical convection[24–27,48–51] indicate that heat transport in a TCBL is very complex. If intrinsic density heterogeneity is large enough for a chemically distinct layer or pile to persist, plumes may rise from a relatively low-temperature boundary layer that is shallower than the CMB. Entrained dense material may cause a plume to founder, preventing its rise through the mantle. If the chemical anomaly has high internal heat production, that contribution to the plume heat flux must be accounted for as well as the CMB heat-flow contribution. Some stratified convection models give an upper bound on CMB heat flow of about 14 TW (ref. 48).

Direct seismological imaging of lower-mantle upwellings provides an alternative approach. Seismic tomography currently achieves spatial resolution on the order of 500–1,000 km throughout most of the mantle. Early estimates of plume radii of 50–100 km suggest that detection of lower-mantle plumes by seismology should not yet be feasible[52]. However, a decrease in thermal expansion with pressure in the deep mantle should produce broader plumes than previously considered, facilitating their detection[53]. Some debated seismic tomography models indicate ~500–1,000 km scale upwellings in the lower mantle beneath some surface hotspots[54,55]. Clustering of upwellings near the margins of large chemically distinct regions in the lowermost mantle[56] may be responsible for very broad regions of low velocity that have been detected extending from the lower mantle into the upper mantle[57].

Interpreting low seismic velocity features in the lower mantle as thermal plumes opens the possibility of estimating buoyancy flux using Stokes' flow models[4]. Estimates of the corresponding heat flux range from 10–30 TW, depending on viscosity. The large radius of the plume-like features in the seismic models is the direct cause of the increase in estimated plume heat flow relative to earlier estimates. Unless a significant amount of internal heating occurs in the deep mantle, corresponding CMB heat-flow values are 3 to 10 times larger than estimates based on dynamic topography. With these numbers it is possible that almost all upward heat transport from the lower mantle to the upper mantle is carried by plumes, which would profoundly change their perceived role in mantle dynamics[4]. However, the low resolution of the seismic models and uncertainty in the viscosity structure[36] and role of chemical heterogeneity motivate additional strategies for estimating the heat flow near the CMB.

POST-PEROVSKITE PHASE TRANSITION

Absolute temperature determinations for the deep Earth are remarkably few in number; until recently, the only precise estimates have been for laboratory-calibrated phase transitions associated with seismologically detected velocity discontinuities at the 410-km and inner core–outer core boundaries[8]. This situation appears to have changed with the discovery of a phase transition of $(Mg,Fe)SiO_3$ perovskite (Pv) — the primary mineral in the lower mantle — to a dense polymorph called post-perovskite (pPv) at pressure and temperature (P–T) conditions within the lowermost mantle[58–60]. The phase change to pPv results in an increase in rigidity, a decrease in incompressibility, and a 1–1.5% increase in density. These, in turn, produce a 2–4% S-wave velocity increase and a weak change (±0.5%) in P-wave velocity[61–63], which are generally consistent with observations of S- and P-wave velocity discontinuities detected several hundred kilometres above the CMB in many locations[64,65].

Theoretical and experimental studies indicate that the Pv-to-pPv phase change has a positive Clapeyron (P–T) slope of 7.5–11.5 MPa K^{-1} (ref. 60), which predicts large depth variations of the shear velocity increase in the presence of strong thermal heterogeneity in the D″ TBL. Seismically observed variations of the D″ discontinuity depth are consistent with a phase change with a large positive Clapeyron slope[66]. Thus, the mineral physics calibration of the absolute P–T position of the phase boundary and its Clapeyron slope can be used as a thermometer, revealing the absolute temperature at the velocity discontinuity. The estimated Pv-to-pPv transition temperature for $MgSiO_3$ is 2,500 K at a pressure of 125 GPa (2,700 km deep in the Earth, 191 km above the CMB)[58]. For comparison, the temperature at 2,700 km depth estimated by extrapolating the mantle potential temperature downward along an adiabat is about 2,700 K (ref. 10), and allowing for ~200 K of subadiabaticity, there is good agreement with the pPv transition temperature, if it is associated with the D″ discontinuity near this depth. Lateral temperature variations of 1,000 K would be expected to give rise to ~10 GPa (200 km) fluctuations in seismic discontinuity depth, comparable to observations[64]. Geodynamical models for whole-mantle convection predict such large thermal variations mainly because of the low temperatures of oceanic slab material penetrating to the lowermost mantle.

Availability of a new *in situ* thermometer in close proximity to the CMB greatly reduces uncertainty in deep-mantle absolute temperatures, as long as variable chemistry does not strongly affect the transition depth[67] and the phase boundary is correctly affiliated with an observed seismic discontinuity. Effects of iron on the transition pressure remain unconstrained owing to uncertainty in experimental pressure standards[68], with conflicting results of both no effect and significant pressure reductions being experimentally and theoretically estimated[60,67]. It is likely that this issue will soon be resolved for moderate (<15%) levels of Fe substitution for Mg, as suggested for the pyrolite model. Seismological mapping of variations in depth of the D″ discontinuity may thus map both the thickness of any pPv layer and the absolute temperature variations[69–74]. The seismic data suggest limited occurrence of thick regions of pPv, which are thought to be confined to the lowest temperature regions beneath circum-Pacific mid-mantle down-wellings. The mapping of discontinuities is quite limited and large low-shear velocity provinces (LLSVPs) at the base of the mantle under the central Pacific and Africa appear to have localized undulating discontinuities on their margins, so it is not

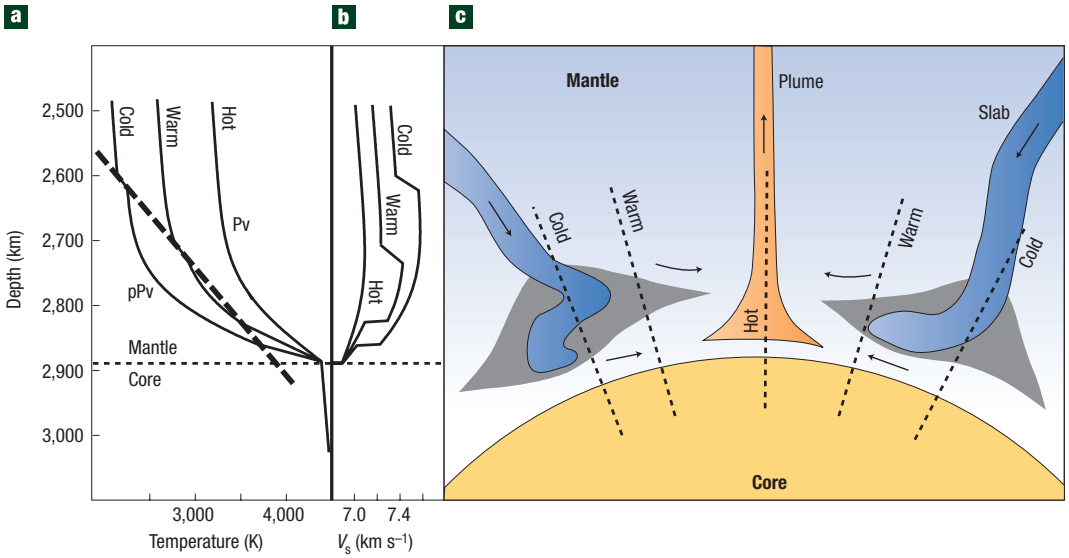

Figure 4 Post-perovskite ocurrence. The presence of the perovskite to post-perovskite phase transition in the lower mantle may account for observed increases in S-wave velocity (V_s) several hundred kilometres above the CMB, and thermal variations may produce the observed topography at the boundary. If the temperature at the CMB exceeds the temperature at which the phase transition boundary intersects the CMB, a double crossing could occur, with reversion to perovskite at the base of the mantle. This could be detected by occurrence of a velocity decrease below the S-velocity increase in D″, and the occurrence of post-perovskite that may pinch out laterally, producing lenses of material (grey zones).

yet possible to constrain the total volume of pPv in the mantle. This does not negate use of the Pv–pPv thermometer where discontinuities are observed.

POST-PEROVSKITE DOUBLE CROSSING

Early *ab initio* estimates of the pPv phase boundary indicated a transition temperature at CMB pressure, T_{pPvCMB}, of ~4,000 K (ref. 59). This value is within the range of recent estimates of T_{CMB} (3,300–4,300 K) inferred from iron melting temperature determinations for the inner-core boundary. This raises the possibility that the lowermost mantle may not be in the pPv stability field; the only way then that pPv could explain the D″ seismic velocity discontinuity is if the TBL geotherm passes into and back out of the pPv stability field at two different depths (Fig. 4). In this context it is important to emphasize that T_{CMB} is essentially a constant[75]. Therefore, if pPv is modulated by pressure and temperature alone, the T_{CMB} determines whether pPv is present in a global layer extending all the way to the CMB or exists within a layer above the CMB bounded above and below by two intersections of the geotherm and the phase boundary. An intriguing possibility of the latter 'double-crossing model'[76] is that the thinned pPv layer in high temperature regions may disappear entirely laterally, yielding lens-like structures of pPv, which explains why D″ discontinuities are not globally detected. The pPv double-crossing is very similar to the kind of structure proposed in thinner and hotter portions of the uppermost mantle where lenses of plagioclase lherzolite may form out of lower-temperature spinel-lherzolite[77].

A prediction of the pPv double-crossing concept is that two seismic discontinuities of opposite sign should be found at the top and bottom of the pPv domain. This should be most readily detected in S-wave velocity structure owing to the large effect of the phase transition. Around the same time as the discovery of pPv, seismic migration studies of D″ beneath Eurasia and the Cocos region were indicating that the D″ shear velocity increase a few hundred kilometres above the CMB is underlain by a velocity decrease 50–100 km above the CMB[78,79]. The basic correspondence with the predictions of the double-crossing model motivated a variety of studies to search for this lower discontinuity and to ensure that it is, indeed, a feature that can be seismically detected[80]. Several recent studies support the existence of paired increases and decreases in velocity compatible with the double-crossing concept[71,72,74,81].

The pPv phase change gives an invaluable absolute temperature at the D″ discontinuity depth, but the double-crossing model (when supported by observed pairs of seismic discontinuities) adds a key second temperature tie-point. This allows thermal models to be fitted to the observations, greatly improving constraints on radial temperature gradients. Using error-function parameterization of the TBL and assuming a thermal conductivity, estimates of the local heat flux can be made. Modelling of paired discontinuity depths under the Central Pacific yields a value of 85 ± 25 m W m^{-2} for the standard, albeit unconstrained, assumption of thermal conductivity, $\kappa = 10$ W m^{-1} K^{-1} (ref.71). Ignoring uncertainty in κ and extrapolating this heat flux over the CMB surface area gives an estimate of 13 ± 4 TW. Similar modelling for the region under the Caribbean yields 35–70 m W m^{-2}, with extrapolation to total CMB heat loss of 7–15 TW for κ = 5–10 W m^{-1} K^{-1} (ref. 74). With pPv expected to occur primarily in the lowest-temperature regions, extrapolated heat-flux estimates may be overestimates.

The double-crossing model raises the possibility that pPv exists in lenses that laterally pinch out and disappear (Fig. 4). An S-wave migration study beneath Eurasia using 15–75 second data reveals lateral disappearance of the upper D″ velocity increase, which is compatible with a laterally limited pPv lens. However, this effect has instead been attributed to lateral chemical variations that induce a broadening of the Pv–pPv two-phase region, which lowers the effective reflectivity of the transition region[70]. Such effects could co-exist with the occurrence of pPv lenses[67].

Existence of pPv double-crossing yields a lower bound for the TBL thermal gradient because this gradient must be steeper than

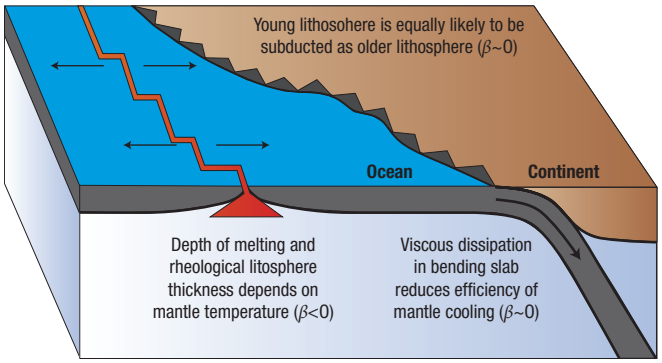

Figure 5 Thermal evolution for plate tectonics. The overall thermal engine of the mantle is likely to differ from that predicted for simple fluid dynamics owing to the dissipation associated with bending of the stiff oceanic lithosphere as it subducts and the complicated pattern of downwellings. Evolution of internal temperatures, volatiles, and depths of melting over time can all affect thermal histories, with the Rayleigh–Nusselt number scaling coefficient having a value near zero rather than near 0.3, as for purely fluid convection. The plate tectonics system thus controls cooling of the mantle and ultimately the heat flow at the CMB.

the phase boundary in order to pass back into the Pv stability field. This minimum thermal gradient is $\rho g/\Gamma$ where ρ is the density, g is gravitational acceleration, and Γ is the pPv Clapeyron slope. A modest increase in the implied thermal gradient beneath a pPv lens relative to the phase boundary alone is required to account for latent heat absorption by material passing downwards and out of the pPv lens[82]. It is important to emphasize that the pPv double-crossing only represents a local heat-flux constraint. Extrapolations to global heat flow are uncertain because it is not known whether pPv is relatively isolated (hence forming unconnected lenses) or if it is abundant (and hence possibly forming a connected layer, perhaps with holes in it) and therefore representative of most of the D″ layer. The proposed presence of a pPv-lens in the generally slower, and presumably warmer, mid-Pacific LLSVP[71] suggests that, with a contribution from chemical modulation of the occurrence of pPv lenses, thermal modelling might still provide an upper bound on global heat flow even if the topology is composed of unconnected lenses.

The pPv double-crossing notion provides a relatively direct method for estimating CMB heat flux, but is subject to uncertainties in thermal conductivity, seismic models, Clapeyron slope, effects of chemical heterogeneity, and amount by which the T_{CMB} exceeds the T_{pPvCMB}. It has been shown that a Clapeyron slope less than about 7–8 MPa K^{-1} is inconsistent with a plausible T_{CMB} and the occurrence of a pPv double-crossing[83], which partially constrains the range of possibilities.

ULTRALOW-VELOCITY ZONES

Very strong seismic velocity reductions have been detected just above the CMB in piles or layers a few tens of kilometres thick[84], with as much as 30% reduction in S-wave velocity (V_s) and 10% reduction in P-wave velocity (V_p). The three times larger decrease in V_s relative to V_p is suggestive of the presence of a mushy zone, and the location just above the CMB suggests that these ultralow-velocity zones (ULVZ) are relatively dense and stable[85]. ULVZs are distinct from the LLSVPs beneath the Pacific and Africa. Proposed mechanisms for the origin of ULVZs range from partial melting of the mantle[85], core–mantle reactions[86], lateral infiltration of core material accommodated by topographic lows in the CMB[87], subduction and segregation of late Archean banded-iron formations[88], upward compaction of sediments crystallizing from the outer core[89], highly Fe-enriched forms of pPv[90], and the mushy residuum of a fractionally crystallized primordial dense melt layer[91].

In the absence of dynamic buoyant flow, a dense basal layer would be expected to flatten out by simple viscous relaxation. Large variations in thickness of a dense basal layer can only be dynamically supported by buoyancy-driven flow[49], and estimates of ULVZ thickness[92] may thus provide a snapshot of dynamics at the base of the Earth's mantle. A simple force balance for thickness variations of 10 km in a ULVZ layer that is 10% denser than surrounding mantle[93] implies variations in dynamic stress on the order of 10 MPa. For an ambient viscosity of 10^{21} Pa s, strain rates on the order of 10^{-14} s^{-1} would be expected in the lowermost mantle. Flows with comparable strain rates can explain the lateral structure of the pPv lens below the mid-Pacific, as inferred from seismic observations[71].

Attributing ULVZs to ongoing partial melting of the mantle is difficult because the required dense melt would tend to percolate downwards and accumulate in a molten layer[94]. Possibly the early deep Earth was warm enough to be in an extensively melted state. If an initially large molten region were denser than solids that crystallize from it during slow cooling[11,95], ULVZs could represent its mushy residuum and would potentially contain a large amount of incompatible heat-producing elements[91]. This model can account for measured differences between $^{142}Nd/^{144}Nd$ abundances in terrestrial samples and chondrites/eucrites[96] if the dense magma layer was formed in the first 100 Myr of Earth history. Despite being model-dependent, the rate of crystallization of the layer can in principle be related to the rate of cooling if the phase diagram is known, which could potentially constrain CMB heat flow in Earth's early history.

If ULVZs contain much of the 'missing' incompatible heat-producing elements, then they could generate about 4–6 TW of radiogenic heat at present[91], similar to crustal values. This power would add to that from cooling of the Earth's core to give the total heat flow to the overlying solid mantle. This would allow a smaller rate of core cooling to be compatible with a relatively high deep-mantle heat flow as indicated by the plume and numerical calculations.

THERMAL HISTORY IMPLICATIONS

Estimates of relatively high heat flow from the lowermost mantle today have implications for conditions during early Earth history, suggesting a high rate of core cooling and the associated late onset of growth of the inner core, a high extent of lower-mantle melting, and substantial evolution of the mantle convective system. It is not difficult to account for high initial core temperatures assuming a significant fraction of the gravitational energy for core formation contributed to superheating of the core as metallic diapirs descended to the Earth's centre. Once the mantle became mostly solid, removal of this heat became sluggish and inefficient. Values of CMB heat flow below ~4 TW can be reconciled with the current energy requirements for the geodynamo and would have permitted the inner core to form early in Earth history. However, larger values of CMB heat flow and larger core dissipation values predict a young (<1 Ga) inner core, which implies that earlier heat-flow values must have been much higher to have sustained a purely thermally driven geodynamo[15,31,97]. Approaches to reconciling this issue tend to invoke radiogenic heat production in either the core or lowermost mantle, as noted above.

The notion that heat-producing elements such as potassium might be soluble in Earth's iron-rich outer core has generated considerable interest[17]. Radiogenic heating lowers internal temperatures when thermal history models are extrapolated back in time. A 250 p.p.m. concentration of potassium in the core — an upper bound associated with high sulphur content in the core— gives about 2 TW of radiogenic

heat, which could be as much as 20% of the higher heat-flow estimates. But, constraints on potassium content are very weak[17]. Alternatively, concentrating heat-producing elements in the lower mantle can modify the CMB TBL, reducing heat flow from the core while still allowing a large heat flux from the deep mantle. The combined effects of reducing the temperature contrast across the TBL and reduced heat conduction down the core adiabat for lower values of core thermal conductivity may allow reasonable core evolution models[37].

The largest source of uncertainty in constructing a reasonable thermal history of the mantle is the rate at which heat is transferred to Earth's surface by mantle convection. Although the present surface cooling rate of ~46 TW is reasonably well-constrained, it is difficult to assess whether this value is representative of the recent geological past, given that fluctuations can occur over timescales of 10^7 to 10^8 years. Further difficulties arise when the heat flow is extrapolated back in time. A key question concerns the relationship between internal temperature and surface heat flux needed to perform thermal history calculations. This relationship is often described by a scaling between the Rayleigh number (Ra), which characterizes the convective vigour, and the Nusselt number (Nu), which is a non-dimensional measure of the heat flow. The scaling is expressed in the form $Ra \approx Nu^{\beta}$, where the value of β in classical Rayleigh–Bènard convection is typically in the range 0.3–0.4. However, mantle convection differs considerably from Rayleigh–Bènard convection. For example, the operation of plate tectonics may cause a large viscous dissipation associated with slab-bending at subduction zones. A scaling law that accounts for this dissipation has $\beta = 0$ (ref. 98). It has been suggested[99] that when Earth was hotter, both melting and effective lithospheric thickness were greater, such that slab-bending was even more inhibitive, leading to a scaling law with $\beta < 0$. A stable equilibrium state cannot be achieved when $\beta < 0$: small perturbations cause the mantle heat transfer rate to depart from any attempted equilibrium with internal heating. More recently, the assumptions of the majority of convective heat transfer models based on boundary layer instability have been questioned[100]. Boundary-layer instability analysis predicts that the lithosphere will subduct once it reaches some critical thickness (or age). However, the age of oceanic lithosphere at subduction zones is presently uniformly distributed. This leads to heat transfer scaling with $\beta = 0$ (Fig. 5) unless the maximum age of oceanic lithosphere varies systematically with mantle temperature.

Improved constraints on the thermal history and current heat-flow balance of the Earth will require sustained multidisciplinary effort, and the heat flux across the CMB will continue to be a focus of attention. Tighter constraints on material properties such as thermal conductivity in the core and mantle are critical. Full characterization of the Clapeyron slope and sensitivity to chemical heterogeneity are needed for the Pv-to-pPv phase transition. Better understanding of dissipation in the geodynamo generation process is needed. More comprehensive seismological characterization of the D″ and core-side boundary layers is required. Higher resolution imaging of deep-mantle velocity heterogeneity and geodynamic modelling of thermal plumes are needed. At present, it appears viable to reconcile the total surface heat flow with chondritic abundances of radiogenic heat-producing elements, but their distribution in the lowermost mantle and core needs further constraints from geochemistry and geodynamics. With all these areas of uncertainty, and possible unrecognized complexity, precision in the estimates of CMB heat flux is not yet in hand.

doi: 10.1038/ngeo.2007.44

References

1. Pollack, H. N., Hurter, S. J. & Johnson, J. R. Heat flow from the Earth's interior: analysis of the global data set. *Rev. Geophys*. **31,** 267–280 (1993).
2. Jaupart, C., Labrosse, S. & Mareschal, J.-C. Temperatures, heat and energy in the mantle of the Earth. *Treatise on Geophys.* (in the press).
3. Kellogg, L. H., Hager, B. H. & van der Hilst, R. D. Compositional stratification in the deep mantle. *Science* **283,** 1881–1884 (1999).
4. Nolet, G., Karato, S.-I. & Montelli, R. Plume fluxes from seismic tomography. *Earth Planet. Sci. Lett.* **248,** 685–699 (2006).
5. Stacey, F. D. & Loper, D. E. The thermal boundary layer interpretation of D″ and its role as a plume source. *Phys. Earth Planet Inter*. **33,** 45–55 (1983).
6. Davies, G. F. Ocean bathymetry and mantle convection. 1. Large-scale flow and hotspots. *J. Geophys. Res*. **93,** 10467–10480 (1988).
7. Sleep, N. H. Hotspots and mantle plumes: some phenomenology. *J. Geophys. Res.* **95,** 6715–6736 (1990).
8. Williams, Q. in *The Core-Mantle Boundary Region* (eds Gurnis, M., Wysession, M. E., Knittle, E. & Buffett, B. A.) 73–81 (AGU, Washington DC, 1998).
9. Holland, K. G. & Ahrens, T. J. Melting of $(Mg,Fe)_2SiO_4$ at the core-mantle boundary of the Earth. *Science* **275,** 1623–1625 (1997).
10. Boehler, R. High-pressure experiments and the phase diagram of lower mantle and core materials. *Rev. Geophys*. **38,** 221–245 (2000).
11. Akins, J. A., Luo, S.-N., Asimow, P. D. & Ahrens, T. J. Shock-induced melting of $MgSiO_3$ perovskite and implications for melts in Earth's lowermost mantle. *Geophys. Res. Lett.* **31,** L14612 (2004).
12. Ahrens, T. J., Holland, K. G. & Chen G. Q. Phase diagram of iron, revised-core temperatures. *Geophys. Res. Lett*. **29,** 1150 (2002).
13. Anderson, O. L. The power balance at the core-mantle boundary. *Phys. Earth Planet. Inter.* **131,** 1–17 (2002).
14. Stacey, F. D. *Physics of the Earth*. 3rd edn (Brookfield Press, Brisbane, Australia, 1992).
15. Buffett, B. A. The thermal state of Earth's core. *Science* **299,** 1675–1676 (2003).
16. Alfe, D. Gillan, M. J. & Price, G. D. Thermodynamics from first principles: temperature and composition of the Earth's core. *Min. Mag*. **67,** 113–123 (2003).
17. Nimmo, F. Core Dynamics: Energetics of the core, in *Treatise on Geophys.* (in the press).
18. Hofmeister, A. M. Mantle values of thermal conductivity and the geotherm from phonon lifetimes. *Science* **283,** 1699–1706 (1999).
19. Stacey, F. D. & Loper, D. E. A revised estimate of the conductivity of iron alloy at high pressure and implications for the core energy balance. *Phys. Earth Planet. Inter.* **161,** 13–18 (2007).
20. Goncharov, A. F., Struzhkin, V. V. & Jacobsen, S. D. Reduced radiative conductivity of low-spin (Mg,Fe)O in the lower mantle. *Science* **312,** 1205–1208 (2006).
21. Lay, T., Williams, Q. & Garnero, E. J. The core-mantle boundary layer and deep Earth dynamics. *Nature* **392,** 461–468 (1998).
22. Wang, Y. & Wen, L. Geometry and P and S velocity structure of the "African Anomaly". *J. Geophys. Res*. 112, B05313 (2007).
23. Simmons, N. A., Forte, A. M. & Grand, S. P. Thermochemical structure and dynamics of the African superplume. *Geophys. Res. Lett*. **34,** L02301 (2007).
24. Farnetani, C. G. Excess temperature of mantle plumes: the role of chemical stratification across D″. *Geophys. Res. Lett*. **24,** 1583–1586 (1997).
25. Tackley, P. J. Mantle convection and plate tectonics: toward an integrated physical and chemical theory. *Science* **288,** 2002–2007 (2000).
26. Montague, N. L. & Kellogg, L. H. Numerical models of a dense layer at the base of the mantle and implications for the geodynamics of D″. *J. Geophys. Res.* **105,** 11101–11114 (2000).
27. Zhong, S. & Hager, B. H. Entrainment of a dense layer by thermal plumes. *Geophys. J. Int.* **154,** 666–676 (2003).
28. McNamara, A. K. & Zhong, S. Thermochemical structures beneath Africa and the Pacific Ocean. *Nature* **437,** 1136–1139 (2005).
29. Namiki, A. & Kurita, K. Heat transfer and interfacial temperature of two-layered convection: Implications for the D″-mantle coupling. *Geophys. Res. Lett*. **30,** 1023 (2003).
30. Stacey, F. D. & Anderson, O. Electrical and thermal conductivities of Fe-Ni-Si alloy under core conditions. *Phys. Earth Planet. Inter*. **124,** 153–162 (2001).
31. Buffett, B. A. Estimates of heat flow in the deep mantle based on the power requirements for the geodynamo. *Geophys. Res. Lett*. **29,** 1555 (2002).
32. Christensen, U. & Tilgner, A. Power requirements of the geodynamo from Ohmic losses in numerical and laboratory dynamos. *Nature* **429,** 169–171 (2004).
33. Glatzmaier, G. & Roberts, P. H. A three-dimensional self-consistent computer simulation of a geomagnetic field reversal. *Nature* **377,** 203–209 (1995).
34. Gubbins, D., Alfe, D., Masters, G., Price, D. & Gillan, M. Gross thermodynamics of 2-component core convection. *Geophys. J. Int*. **157,** 1407–1414 (2004).
35. Nakagawa, T. & Tackley, P. J. Deep mantle heat flow and thermal evolution of the Earth's core in thermochemical multiphase models of mantle convection. *Geochem. Geophys. Geosyst*. **6,** Q08003 (2005).
36. Korenaga, J. Firm mantle plumes and the nature of the core-mantle boundary region. *Earth Planet. Sci. Lett*. **232,** 29–37 (2005).
37. Davies, G. F. Mantle regulation of core cooling: A geodynamo without core radioactivity? *Phys. Earth Planet. Inter*. **160,** 215–229 (2007).
38. Nimmo, F., Price, G. D., Brodholt, J. & Gubbins, D. The influence of potassium on core and geodynamo evolution. *Geophys. J. Int*. **156,** 363–376 (2004).
39. Lister, J. R. & Buffett, B. A. Stratification of the outer core at the core-mantle boundary. *Phys. Earth Planet. Int.* **105,** 5–19 (1998).
40. Helffrich, G. & Kaneshima, S. Seismological constraints on core composition from Fe-O-S liquid immiscibility. *Science* **306,** 2239–2242 (2004).
41. Eaton, D. W. & Kendall, J.-M. Improving seismic resolution of outermost core structure by multichannel analysis and deconvolution of broadband SmKS phases. *Phys. Earth Planet. Inter.* **155,** 104–119 (2006).
42. Tanaka, S. Seismic detectability of anomalous structure at the top of the Earth's outer core with broadband array analysis of SmKS phases. *Phys. Earth Planet. Int.* **141,** 141–152 (2004).
43. Gubbins, D. Geomagnetic constraints on stratification at the top of Earth's core. *Earth Planets Space* **59,** 661–664 (2007).
44. Davies, G. F. Cooling the core and mantle by plume and plate flows. *Geophys. J. Int*. **115,** 132–146 (1993).

45. Mittelstaedt, E. & Tackley, P. Plume heat flow is much lower than cmb heat flow. *Earth Planet. Sci. Lett.* **241,** 202–210 (2006).
46. Labrosse, S. Hotspots, mantle plumes and core heat loss. *Earth Planet. Sci. Lett.* **199,** 147–156 (2002).
47. Behn, M., Conrad, C. & Silver, P. Detection of upper mantle flow associated with the African superplume. *Earth Planet. Sci. Lett.* **224,** 259–274 (2004).
48. Zhong, S. Constraints on thermochemical convection of the mantle from plume heat flux, plume excess temperature, and upper mantle temperature. *J. Geophys. Res.* **111,** B04409 (2006).
49. Jellinek, A. M. & Manga, M. The influence of a chemical boundary layer on the fixity, spacing and lifetime of mantle plumes. *Nature* **418,** 760763 (2002).
50. Nakagawa, T. & Tackley, P. J. Effects of thermo-chemical mantle convection on the thermal evolution of the Earth's core. *Earth Planet Sci. Lett.* **220,** 107–119 (2004).
51. Tan, E. & Gurnis, M. Compressible thermochemical convection and application to lower mantle structures. *J. Geophys. Res.* **112,** B06304 (2007).
52. Nataf, H.-C. Seismic imaging of mantle plumes. *Annu. Rev. Earth Planet. Sci.* **28,** 319–417 (2000).
53. Goes, S. Cammarano, F. & Hansen, U. Synthetic seismic signature of thermal plumes. *Earth Planet. Sci. Lett.* **218,** 403–419 (2004).
54. Zhao, D. Seismic structure of hotspots and mantle plumes. *Earth and Planet. Sci. Lett.* **192,** 251–265 (2001).
55. Montelli, R., Nolet, G., Dahlen, F. A., Masters, G. Engdahl, E. R. & Hung, S.-H. Finite-frequency tomography reveals a variety of plumes in the mantle. *Science* **303,** 338–343 (2004).
56. Thorne, M. S., Garnero, E. J. & Grand, S. P. Geographic correlation between hotspots and deep mantle lateral shear-wave velocity gradients. *Phys. Earth Planet. Inter.* **146,** 47–63 (2004).
57. Romanowicz, B. & Gung, Y. C. Superplumes from the core-mantle boundary to the lithosphere: implications for heat flux. *Science* **296,** 513–516 (2002).
58. Murakami, M., Hirose, K., Kawamura, K. Sato, N & Ohishi, Y. Post-perovskite phase transition in $MgSiO_3$. *Science* **304,** 855–858 (2004).
59. Oganov, A. R. & Ono, S. Theoretical and experimental evidence for a post-perovskite phase of $MgSiO_3$ in Earth's D″ layer. *Nature* **430,** 445–448 (2004).
60. Hirose, K. Postperovskite phase transition and its geophysical implications. *Rev. Geophys.* **44,** RG3001 (2006).
61. Stackhouse, S., Brodholt, J. P., Wookey, J., Kendall, J.-M. & Price, G. D. The effect of temperature on the seismic anisotropy of the perovskite and post-perovskite polymorphs of $MgSiO_3$. *Earth Planet. Sci. Lett.* **230,** 1–10 (2005).
62. Wentzcovitch, R. M., Tsuchiya, T. & Tsuchiya, J. $MgSiO_3$ postperovskite at D″ conditions. *Proc. Nat. Acad. Sci. USA* **103,** 543–546 (2006).
63. Wookey, J., Stackhouse, S., Kendall, J.-M., Brodholt, J. & Price, G. D. Efficacy of post-perovskite as an explanation for lowermost mantle seismic properties. *Nature* **438,** 1004–1007 (2005).
64. Wysession, M. E. *et al.* in *The Core-Mantle Boundary Region*. (eds Gurnis, M., Wysession, M. E., Knittle, E. & Buffett, B. A.) 273–297 (AGU, Washington DC, 1998).
65. Lay, T. & Garnero, E. J. in *Post-perovskite: The Last Phase Change*. (eds Hirose, K., Brodholt, J., Lay, T. & Yuen D.) (AGU, in the press).
66. Sidorin, I., Gurnis, M. & Helmberger, D. V. Evidence for a ubiquitous seismic discontinuity at the base of the mantle. *Science* **286,** 1326–1331 (1999).
67. Spera, F. J., Yuen, D. A. & Giles, G. Tradeoffs in chemical and thermal variations in the post-perovskite phase transition: Mixed phase regions in the deep lower mantle? *Phys. Earth Planet. Inter.* **159,** 234–246 (2006).
68. Hirose, K. Sinmyo, R., Sata, N. & Ohishi, Y. Determination of post-perovskite phase transition boundary in $MgSiO_3$ using Au and MgO pressure standards. *Geophys. Res. Lett.* **33,** L01310 (2006).
69. Helmberger, D. V., Lay, T., Ni, S. & Gurnis, M. Deep mantle structure and the post-perovskite phase transition. *Proc. Natl Acad. Sci. USA* **102,** 17257–17263 (2005).
70. Chambers, K. & Woodhouse, J. H. Transient D″ discontinuity revealed by seismic migration. *Geophys. Res. Lett.* **33,** L17312 (2006).
71. Lay, T., Hernlund, J., Garnero, E. J. & Thorne, M. S. A post-perovskite lens and D″ heat flux beneath the central Pacific. *Science* **314,** 1272–1276 (2006).
72. Sun, D., Song, T.-R. A. & Helmberger, D. Complexity of D″ in the presence of slab-debris and phase changes. *Geophys. Res. Lett.* **33,** L12S07 (2006).
73. Sun, D. Tan, E., Helmberger, D. & Gurnis, M. Seismological support for the metastable superplume model, sharp features, and phase changes within the lower mantle, *Proc. Natl Acad. Sci. USA* **104,** 9151–9155 (2007).
74. van der Hilst, R. D., de Hoop, M. V., Wang, P., Shim, S.-H., Ma, P. & Tenorio, L. Seismostratigraphy and thermal structure of Earth's core-mantle boundary region. *Science* **315,** 1813–1817 (2007).
75. Braginski, S. I. & Roberts, P. H. Equations governing convection in Earth's core and the geodynamo. *Geophys. Astrophys. Fluid Dyn.* **79,** 1–97 (1995).
76. Hernlund, J. W., Thomas, C. & Tackley, P. J. A doubling of the post-perovskite phase boundary and structure of the Earth's lowermost mantle. *Nature* **434,** 882–886 (2005).
77. Kaus, B. J. P., Connolly, J. A. D., Podladchikov, Y. Y. & Schmalholz, S. M. The effect of mineral phase transitions on sedimentary basic subsidence and uplift. *Earth Planet. Sci. Lett.* **233,** 213–228 (2005).
78. Thomas, C., Garnero, E. J. & Lay, T. High-resolution imaging of lowermost mantle structure under the Cocos plate. *J. Geophys. Res.* **109,** B08307 (2004).
79. Thomas, C., Kendall, J.-M. & Lowman, J. Lower-mantle seismic discontinuities and the thermal morphology of subducted slabs. *Earth Planet. Sci. Lett.* **225,** 105–113 (2004).
80. Flores, C. & Lay, T. The trouble with seeing double. *Geophys. Res. Lett.* **32,** L24305 (2005).
81. Avants, M. Lay, T., Russell, S. A. & Garnero, E. J. Shear velocity variation within the D″ region beneath the central Pacific. *J. Geophys. Res.* **111,** B05305 (2006).
82. Buffett, B. A. Bounds on heat flow beneath a double crossing of the perovskite-postperovskite phase transition. *Geophys. Res. Lett.* (submitted).
83. Hernlund, J. W. & Labrosse, S. Geophysically consistent values of the perovskite to post-perovskite transition Clapeyron slope. *Geophys. Res. Lett.* **34,** L05309 (2007).
84. Garnero, E. J., Revenaugh, J., Williams, Q., Lay, T. & Kellogg, L. H. in *The Core-Mantle Boundary Region* (eds Gurnis, M., Wysession, M. E., Knittle, E. & Buffett, B. A.) 319–334 (AGU, Washington DC, 1998).
85. Williams, Q. & Garnero E. J. Seismic evidence for partial melt at the base of the Earth's mantle. *Science* **273,** 1528–1530 (1996).
86. Knittle, E. & Jeanloz, R. The Earth's core–mantle boundary: results of experiments at high pressures and temperatures. *Science* **251,** 1438–1443 (1991).
87. Kanda, R. V. S. & Stevenson, D. J. Suction mechanism for iron entrainment into the lower mantle. *Geophys. Res. Lett.* **33,** L02310 (2006).
88. Dobson, D. P. & Brodholt, J. P. Subducted banded iron formations as a source of ultralow-velocity zones at the core-mantle boundary. *Nature* **434,** 371–373 (2005).
89. Buffett, B. A., Garnero, E. J. & Jeanloz, R. Sediments at the top of Earth's core. *Science* **290,** 1338–1342 (2000).
90. Mao, W. L. *et al.* Iron-rich post-perovskite and the origin of ultralow-velocity zones. *Science* **312,** 564–565 (2006).
91. Labrosse, S., Hernlund, J. W. & Coltice, N. A crystallising dense magma ocean at the base of the Earth's mantle. *Nature* (in the press).
92. Thorne, M. S. & Garnero, E. J. Inferences on ultra-low velocity zone structure from a global analysis of SPdKS waves. *J. Geophys. Res.* **109,** B08301 (2004).
93. Rost, S., Garnero, E. J., Williams, Q. & Manga, M. Seismic constraints on a possible plume root at the core-mantle boundary. *Nature* **435,** 666–669 (2005).
94. Hernlund, J. & Tackley, Some dynamical consequences of partial melting in Earth's deep mantle. *Phys. Earth Planet. Inter.* (in the press).
95. Stixrude, L. & Karki, B. Structure and freezing of $MgSi0_3$ liquid in Earth's lower mantle. *Science* **310,** 297–299 (2005).
96. Boyet, M. & Carlson, R. ^{142}Nd evidence for early (> 4.53 Ga) global differentiation of the silicate Earth. *Science* **309,** 576–581 (2005).
97. Labrosse, S., Poirier, J.-P. & Le Mouel, J.-L. The age of the inner core. *Earth Planet. Sci. Lett.* **190,** 111–123 (2001).
98. Conrad, C. P. & Hager, B. H. Thermal evolution of an Earth with strong subduction zones. *Geophys. Res. Lett.* **26,** 3041–3044 (1999).
99. Korenaga, J., Energetics of mantle convection and the fate of fossil heat. *Geophys. Res. Lett.* **30,** 1437 (2003).
100. Labrosse, S. & Jaupart, C. The thermal evolution of the Earth: Long term and fluctuations. *Earth Planet. Sci. Lett.* (in the press).

Acknowledgements

We thank F. Nimmo and S. Labrosse for preprints, and F. Nimmo, Richard Holme and Bill McDonough for their comments on the manuscript. T.L.'s research on the deep Earth is supported by the NSF. Supplementary Information is linked to the online version of the paper at www.nature.com/nature.

Author contributions

T.L., J.H. and B.A.B. contributed equally to the writing, data analysis and ideas in this paper.